Applied Surface Science 313 (2014) 424–431

Contents lists available at ScienceDirect

Applied Surface Science

journal homepage: www.elsevier.com/locate/apsusc

First principles study on the adsorption of Pt_n (n = 1–4) on γ-Al_2O_3(1 1 0) surface

Yulu Liu [a], Wanglai Cen [a,b,*], Gang Feng [c,*], Yinghao Chu [a], Dejin Kong [c], Huaqiang Yin [a,b,d]

[a] College of Architecture and Environment, Sichuan University, Chengdu 610065, PR China
[b] National Engineering Center of Flue Gas Desulfurization, Chengdu 610065, PR China
[c] Shanghai Research Institute of Petrochemical Technology SINOPEC, Shanghai 201208, PR China
[d] Institute of New Energy and Low Carbon Technology, Sichuan University, Chengdu 610065, PR China

ARTICLE INFO

Article history:
Received 28 April 2014
Received in revised form 30 May 2014
Accepted 30 May 2014
Available online 6 June 2014

Keywords:
Pt cluster
Alumina
Density functional theory
Hydrogen spillover

ABSTRACT

The density functional theory (DFT) was applied to investigate the adsorption and growth of Pt_n (n = 1–4) clusters and hydrogen spillover on γ-Al_2O_3 surface, which is of importance for many catalysis reactions. It was found that the growth ability of the supported Pt_n cluster is weaker than the gas phase Pt_n clusters. Basin structures on both of the clean and hydrated surfaces were found to stabilize the Pt clusters. For the hydrated surface, the basin structure, together with the size of Pt_n cluster, was also found to take trivial impacts on the hydrogen spillover. The most feasible supplier of H species on the hydrated γ-Al_2O_3 surface was identified. Additionally, it was interesting to found that there would be an optimized size of the supported Pt_n cluster at n > 3.

1. Introduction

Noble metals supported on oxides like CeO_2 [1], ZrO_2 [2] and γ-Al_2O_3 [3–5] are versatile catalysts widely used both in traditional fields such as petrochemicals and oil refining [6], and new areas including catalytic purification of vehicle exhaust and volatile organic pollutions [7–9]. The catalytic activity is intrinsically related to the transfer of H species such as hydrogenation and dehydrogenation [10]. An important and interesting related process is well known as hydrogen spillover, which has been found on catalyst Pt/γ-Al_2O_3 [11,12]. Although it is well accepted that the hydrogen spillover is dependent on the chemical nature and texture of noble metal cluster and oxide support, and the complicated interaction between the two [13,14], a deep understanding of the atomistic picture is still limited.

The size and shape of Pt cluster dispersed on supports has been investigated extensively. For traditional petrochemicals and oil refining, the size of Pt cluster was characterized to be 0.8–1 nm [7]. It is corresponding to Pt cluster with 10–20 atoms and has been used in a lot of works [1,7,15]. Smaller Pt_n (n < 10) cluster should be much more active [16], which meets the need of environmental catalysis for purification of dilute pollutions (~0.1 vol.%). A Pt_4 supported on CeO_2 has been reported by Nguyen et al. [17]. Sintering from Pt to Pt_4 on dehydrated γ-Al_2O_3(1 0 0) has been investigated by Mei et al. [18]. The details of the interaction between small Pt_n clusters and the support, and the activity of hydrogen spillover, are still open questions.

The unique properties of acid-basic nature of the support γ-Al_2O_3 possesses an important impact on the stability and growth of active cluster, and further on catalytic reactions taking place on it [19,20]. It has long been an open question of the surface model, as it is alternatively shifted between hydrated and clean states under realistic reaction conditions, which results in modifying of surface geometric and chemical nature [3,13,19–22]. Based on DFT calculations, Li et al. [23] declared that single Cu atom located on hydrated γ-Al_2O_3(1 1 0) surface was more stable than that on clean surface due to the difference in Cu-support interactions. While for Cu_n (n = 2–4), the order is reversed. The aggregations of single Cu and Pd were found to be thermodynamically unfavorable inhibited by the penta-coordinated Al^{3+} sites of dehydrated γ-Al_2O_3(1 0 0) surface [18,23]. Comparing to dehydrated surface, the hydration of γ-Al_2O_3 surfaces inhibited the growth of Cu cluster [23], while favored the growth of Rh cluster [24]. These results indicate that the rules of the adsorption and growth of metal cluster depend on the nature of metal species and the support.

* Corresponding author at: College of Architecture and Environment, Sichuan University, Chengdu 610065, PR China. Tel.: +86 13488962989.
E-mail addresses: cenwanglai@scu.edu.cn (W. Cen), fengg.sshy@sinopec.com (G. Feng).

http://dx.doi.org/10.1016/j.apsusc.2014.05.226
0169-4332/

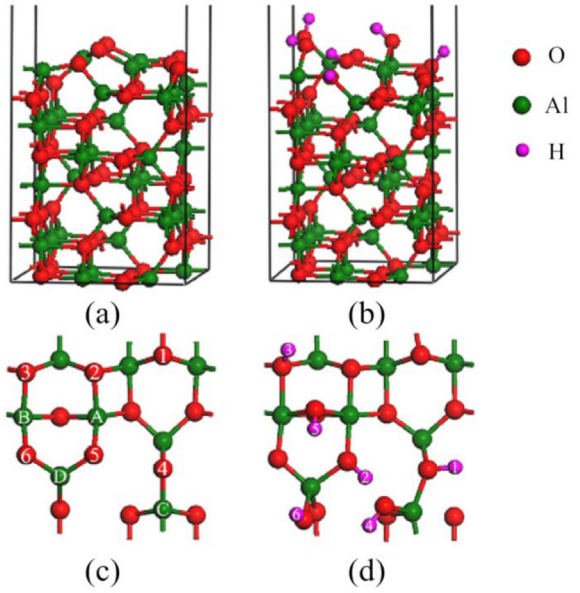

Fig. 1. Converged slab models of clean γ-Al_2O_3(1 1 0) (a, denoted as C_Al_2O_3) and hydrated γ-Al_2O_3(1 1 0) (b, denoted as H_Al_2O_3) surfaces. (c) and (d) are the top view of (a) and (b), respectively.

It was also found the hydroxylation of γ-Al_2O_3 surface have different effects to various catalytic processes. Typically for CO_2 catalytic hydrogenation, surface hydroxyls were found to alter the pathway and selectivity to the product formate or CO for catalyst Ni/γ-Al_2O_3 [13]. While, it has few effects on the distribution of final products and selectively to formate on Cu/γ-Al_2O_3 [25]. The hydroxylation may weaken the CO_2 chemisorption [26], but can help to stabilize the Co–Cu interfacial structure and result in an asymmetrically activated CO_2 adsorption complex [22].

In the present work, we focus on the adsorption and growth of small Pt_n (n = 1–4) clusters on the γ-Al_2O_3(1 1 0) model surfaces proposed by Digne et al. [19,20]. The sites dependence of hydrogen spillover on Pt_n/γ-Al_2O_3 model catalyst is also investigated for the hydrated surface.

2. Model and methods

The Digne's γ-Al_2O_3(1 1 0) surface model was used to descript the alumina surface [19], which accounts for more than 70% of the exposed surface of γ-Al_2O_3 under real catalytic conditions. The $p(1 \times 1)$ eight-layer slab (8.40×8.07 Å^2) consists of sixteen Al_2O_3 units with a 15 Å vacuum zone in the z direction. The four outmost layers of the slabs were fully relaxed, with the four bottom layers fixed in their bulk position. The clean γ-Al_2O_3 (1 1 0) surface (denoted as C_Al_2O_3) is shown as Fig. 1a, with the topmost atoms labeled and shown as Fig. 1c. The hydrated γ-Al_2O_3(1 1 0) surface (denoted as H_Al_2O_3) was fabricated by introducing three H_2O molecules, which were dissociated and located on the C_Al_2O_3 surface to form six OH groups. Among them, the OH groups 1–3 are derived from hydrogenation of lattice oxygen atoms. And the other three OH group 4–6 are parts of H_2O molecules and adsorbed on surface Al cations. This hydrated surface, with a hydroxyl surface coverage 8.9 OH nm^{-2}, has been described in the previous works [19,27,28].

Periodic DFT calculations were performed with spin polarized GGA + PBE [29] exchange-correlation functional as implemented in the code VASP 5.2 [30,31]. The projected augmented wave method [32] was used to describe the core-electron interactions and the Kohn-Sham wave functions were expanded in the plane wave basis

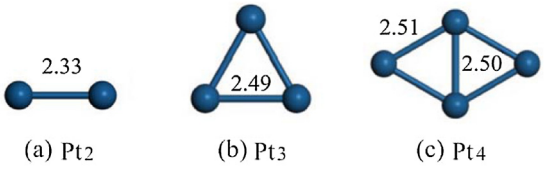

Fig. 2. Converged configurations of isolated Pt_n (n = 2–3) clusters. Selected bond lengths are labeled in Å.

with a kinetic energy cutoff of 400 eV. Gaussian smearing method with a width 0.2 eV was used to determine the partial occupancies. The Brillouin zone was sampled with a $3 \times 3 \times 1$ k-points mesh for the $p(1 \times 1)$ supercell, generated by the Monkhorst–Pack algorithm. The Hellmann–Feynman forces for all relaxed atoms were converged to 0.03 eV/Å. The freestanding Pt clusters in different sizes were calculated in a cubic box with side length 15 Å with a single k-point. The adsorption energy is defined as

$$\Delta E_{ads} = E\left(\frac{M}{slab}\right) - [E(M) + E(slab)] \quad (1)$$

where the E(M/slab), E(M) and E(slab) are the total energies of the slab with adsorbed species, the isolated Pt_n cluster, and the slab of clean or hydrated γ-Al_2O_3 surface, respectively.

During the adsorption of M on slab, both the M and the slab will be reconstructed to new conformations M' and slab′, respectively. Such reconstructions result in decrease of total energy, while increase for each of the M and slab. Based on this, the deformation energy for "M" and "slab" are defined as

$$E_{def,M} = E(M') - E(M) \quad (2)$$

$$E_{def,slab} = E(slab') - E(slab) \quad (3)$$

Finally, the cluster–support interaction energy, E_{int}, is defined as

$$E_{int} = E\left(\frac{M}{slab}\right) - [E(M') + E(slab')] \quad (4)$$

From Eqs. (1)–(4), it can be deduced that $E_{int} = \Delta E_{ads} - (E_{def,M} + E_{def,slab})$. The cluster–support interaction energy of the cluster adsorption process is consumed partially by deformation of M and slab. The rest is released as adsorption energy.

3. Results

3.1. Pt_n clusters

At first, we study the geometries and binding energies of isolated Pt_n clusters, which are the basis to investigate the growth of Pt_n cluster on clean or hydrated γ-Al_2O_3 surfaces. Different initial configurations of Pt_n (n = 2–4) clusters have been checked, and only the most stable (with the lowest total energy) relaxed configurations are reported. The converged Pt_3 is a regular triangle with all the three bond lengths 2.49 Å, elongated from 2.33 Å of Pt_2 by 0.16 Å. For the most stable configuration of Pt_4, the four Pt atoms are in a plane, with equivalent length of side 2.51 Å. The average Pt—Pt bond length $\bar{d}$(Pt—Pt) of Pt_n clusters increase monotonically, from 2.33 to 2.51 Å. But, they are lower than the calculated bulk value 2.78 Å, which is equal to the experimental value as reported in Ref. [33]. Both the values and the trend are consistent with the work of Sanchez et al. [34] (Fig. 2).

To evaluate the stability of isolated clusters, we define the binding energy of Pt_n cluster $E_{bind}(Pt_n) = [n \times E(Pt) - E(Pt_n)]/n$, where $E(Pt_n)$ and $E(Pt)$ are the total energies of the isolated Pt_n cluster (n = 2–4) and the single Pt atom, respectively. The binding energies are 1.84, 2.41 and 2.70 eV, respectively, for n = 2–4. Consequently,

Table 1
Energies (eV), average bond lengths (Å) and Bader valences (BV, e) of the most stable adsorption configurations of Pt_n cluster on C_Al_2O_3 surface.

n	E_{ads}	E_{int}	$E_{def,Ptn}$	$E_{def,surface}$	$\bar{d}$(Pt—Pt)	BV[a]
1	−2.62	−3.34	0	0.72	–	−0.245
2	−3.29	−4.77	0.11	1.37	2.45	−0.345
3	−4.16	−6.06	0.01	1.89	2.52	−0.440
4	−4.78	−8.21	1.02	2.41	2.57	−0.529

[a]The Bader valence (BV) was defined as: BV = bader population [38]–valence charges of Pt_n. Negative means Pt_n cluster accepts electrons from the surface.

Table 2
Selected energies (eV), average bond length (Å) and Bader valences (BV, e) of the most stable adsorption configurations of Pt_n cluster on H_Al_2O_3 surface.

n	E_{ads}	E_{int}	$E_{def,Ptn}$	$E_{def,surface}$	$\bar{d}$(Pt—Pt)	BV
1	−1.88	−2.86	–	0.98	–	−0.226
2	−1.99	−3.93	0.13	1.81	2.46	−0.300
3	−3.51	−5.79	0.01	2.27	2.49	−0.399
4	−3.54	−6.38	0.36	2.48	2.60	−0.407

both the Pt—Pt bond length and binding energy of Pt_n clusters increase with the increase of cluster size. This trend is consistent with isolated Pd_n [35] and Ni_n [36] clusters. It should be ascribed to the increase of coordinate number of Pt_n that helps to stabilize each Pt atom.

3.2. Pt_n adsorption on γ-Al_2O_3 surfaces

As shown in Fig. 1c of the C_Al_2O_3 surface, the four cationic Al sites labeled as A-D are the Lewis acidic sites. The unique Al atom at site D (denoted as Al_D) is the only tri-coordinated surface cation and the other three are tetra-coordinated. According to published works [19,37], the Al_D site should be facile for the localization of electron donating groups, for instance, metal clusters, due to its strong Lewis acidity. The geometric "basin" Al_C-Al_D-O_5-O_4 is appropriate for the location of small Pt_n cluster for its low steric hindrance. Due to Lewis acidity of the Al (A-D) sites of C_Al_2O_3, they are prior to grasp OH groups to form the H_Al_2O_3 surface (Fig. 1d) during surface hydration in realistic reaction. The Pt_n cluster may trend to be loaded on the new basin O_1-Al_A-O_4-Al_B, as promoted in previous published works [16]. Both of these two situations will be investigated.

3.2.1. Pt_n adsorption on the clean surface

The most stable configurations of Pt_n (n = 1–4) adsorption on C_Al_2O_3 surface are shown as Fig. 3a–d. It shows that all the clusters are accommodated in the basin structure Al_C-Al_D-O_5-O_4. In fact, the Al_C-Al_D-O_5-O_4 is part of the whole basin Al_C-O_2-Al_D-O_5-O_4 as shown in Fig. 3b–d. The single Pt atom is localized in the upper part of the basin, coordinated by Al_C, Al_D, O_5 and O_4 atoms. While for n = 2–3, the Pt_n clusters occupy the entire basin and keep in its isolated conformation with few changes, except for Al_C, Al_D, O_5 and O_4 atoms, it is also coordinated to O_2 atom. While for n = 4 as shown in Fig. 3d, the conformation of Pt_n cluster is changed from equilateral quadrilateral in plane to three dimensional tetrahedron. The atom Pt_2 of the cluster Pt_4 is even extruded out of the basin and coordinated to O_3 atom.

Correspondingly, the interaction energies E_{int} increase monotonically from −3.34 to −8.21 eV, with the increase of the Pt_n cluster sizes (see Table 1). According to the definition of different energy items mentioned in Section 2, the interaction energy is split into adsorption energy, the deformation energies of the C_Al_2O_3 surface and the supported Pt_n clusters. As listed in Table 1, most of the energy is released as adsorption energy E_{ads}. Then, it is the deformation of the non-hydrated slab surface.

The distances between Pt atoms in the adsorbed clusters became longer than their isolated counterparts. For Pt_2 and Pt_4, they are elongated from 2.33 and 2.51 Å to 2.45 and 2.57 Å, respectively. For the Pt_4 cluster, the drastic changes in conformation make the deformation energy as high as 1.02 eV. While for Pt_3, the elongation of Pt—Pt distances is quite trivial, which makes the deformation energy as low as 0.01 eV. The unusual reduce of deformation energy of Pt_n (n = 3) has also been reported for Cu_n and Pd_n (n = 3) on hydrated γ-Al_2O_3 surface [23,35]. All the Bader valences are negative, increased from −0.245 to −0.529 eV, indicating that more electrons were transferred from the slab surface to the supported Pt_n clusters as the cluster size increases.

3.2.2. Pt_n adsorption on the hydrated surface

The most stable configurations of Pt_n (n = 1–4) adsorption on H_Al_2O_3 surface are shown as Fig. 3e–h. All the clusters are accommodated in the basin structure O_1-Al_A-O_4-Al_B. For n = 1, the single atom Pt is coordinated to O_1 atom (Fig. 3e). For n = 2–4, all the conformations of the adsorbed Pt_n are similar to their isolated counterparts. Particularly for n = 4, the Pt_n is still in quadrilateral conformation, even though it does not keep in plane structure (Fig. 3h).

Related energy items were collected in Table 2. Similar to their counterparts on clean surfaces, both the adsorption energies and interaction energies increased with the increase of cluster size. While, the absolute values on the hydrated surfaces are smaller than that on the clean surface, correspondingly. The deformation energy ($E_{def,surface}$) of the H_Al_2O_3 surface is also increased as the size of Pt_n increase, from 0.98 to 2.48 eV. Each of the values is larger than their counterparts of C_Al_2O_3. These energetic results indicate that the hydration of the surface not only weakens the metal–support interaction, but also reduces the proportion of adsorption energy. The same effects of surface hydroxylation have been reported in the previous works [23,35,36]. It could be ascribed to that hydration helps to reduce the unsaturated coordination of the raw cleaved surface and makes the surface much more flexible. The deformation energies of supported Pt_2 and Pt_3 clusters are quite equivalent to that on C_Al_2O_3. However, the deformation energy of Pt_4 is 0.36 eV, which is one third of that on C_Al_2O_3. It indicates the deformation of Pt_4 supported on H_Al_2O_3 is less than that on C_Al_2O_3.

Bader analysis indicates the adsorbed Pt_n clusters accept electrons from the hydrated surfaces, and the BV increases as the increase of the Pt_n size. This trend is the same to that on non-hydrated surface, while the BV of the former is smaller than that of the latter. It is consistent with the decrease of interaction energy.

3.2.3. Growth of Pt_n clusters

In this section, we further study the growth of free Pt_n cluster and Pt_n cluster supported on γ-Al_2O_3(1 1 0) surfaces. The growth energy (E_{grow}) on surface is defined as [24]:

$$E_{grow} = E\left(\frac{Pt_n}{\gamma\text{-}Al_2O_3}\right) + E(\gamma\text{-}Al_2O_3) - E\left(\frac{Pt_{n-1}}{\gamma\text{-}Al_2O_3}\right) - E\left(\frac{Pt_1}{\gamma\text{-}Al_2O_3}\right) \quad (5)$$

While for the isolated cluster, it is simplified as:

$$E_{grow} = E(Pt_n) - E(Pt_{n-1}) - E(Pt_1) \quad (6)$$

All the growth energies of Pt_n cluster are plotted in Fig. 4. It shows that the growth of Pt_n (n = 2–4) cluster is thermodynamically favorable and exothermic since all the growth energies are minus. Totally, the growth trend of Pt_n cluster is as: Pt_n/C_Al_2O_3 < Pt_n/H_Al_2O_3 < isolated Pt_n. No matter hydrated or not, the support can act as a stabilizer of the metal cluster and

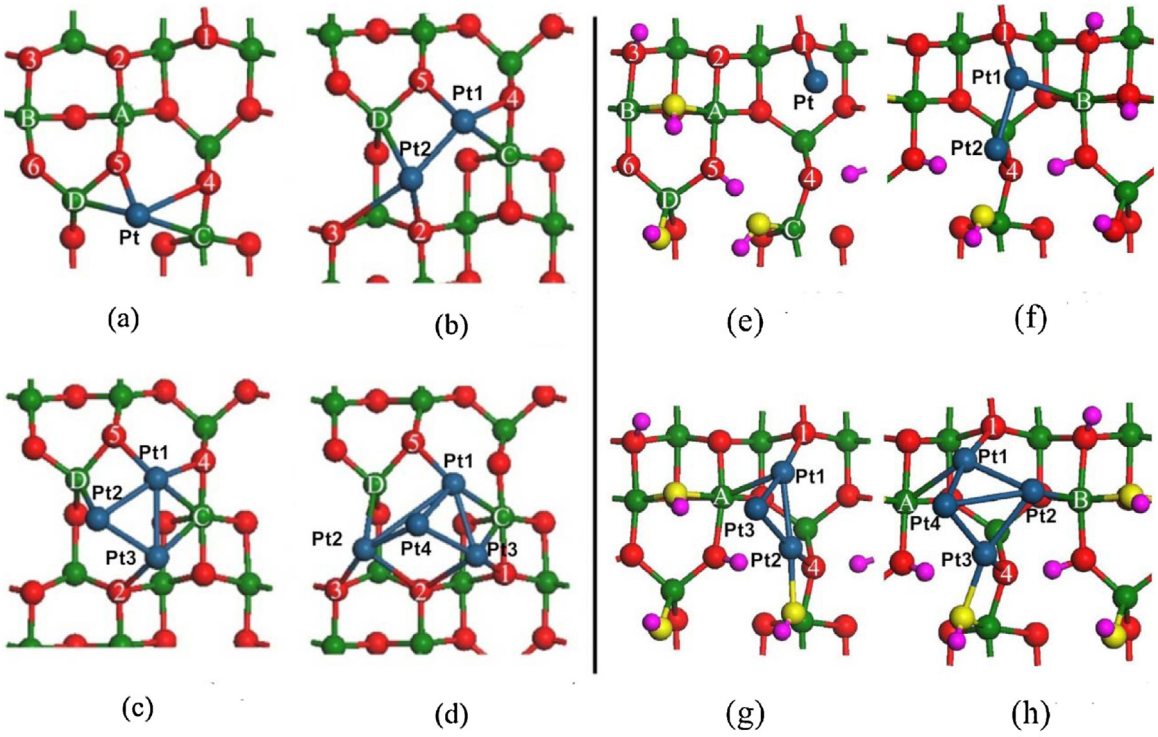

Fig. 3. The most stable adsorption configurations of Pt_n (n = 1–4) clusters on C_Al_2O_3 (a-d) and H_Al_2O_3 (e-h) surfaces. Bond lengths are in Å. Blue ball: Pt atom; yellow ball: O atom originated from dissociation of H_2O molecule; the others are the same to Fig. 1.

the hydroxylation of surface reduces the contribution to the stabilization. It is consistent with published works for Ni_n and Pd_n supported on γ-Al_2O_3(1 1 0) [35,36,39]. Meanwhile, the curves of growth energy of Pt_n cluster on γ-Al_2O_3(1 1 0) surfaces have a turning point at n = 2–3. It indicates that there should be an upper size limitation of the surface basin to accommodate a Pt_n cluster.

3.3. Hydrogen spillover

Hydrogen spillover energy (E_{sp}) is defined as:

$$E_{sp} = E\left(Pt_n/Al_2O_3\right)^* - E\left(Pt_n/Al_2O_3\right) \quad (7)$$

where $E(Pt_n/Al_2O_3)^*$ is the total energy of Pt_n/Al_2O_3 after spillover.

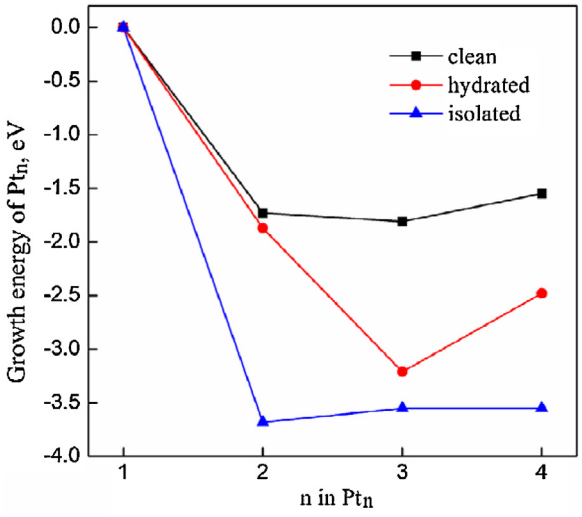

Fig. 4. The curves of growth energies of Pt_n cluster supported on γ-Al_2O_3(1 1 0) surfaces and isolated Pt_n cluster.

The most preferable pathway of hydrogen spillover on Pt_1/H_Al_2O_3 is presented in Fig. 5. The Pt located at site O_1 inserted into the H—O bond at site 3, with 1.17 eV released, which is exothermic. The net energy cost for the spilled H3 atom desorption as $1/2H_2$ is 0.28 eV. A further desorption of H5 as $1/2H_2$ is unfeasible as additional 0.8 eV will be exhausted. It should be noted that, the energy reduction is quite considerable (1.17 eV) for the initial H spillover, which takes account of the high activity of single atom dispersed Pt supported catalysts. Several other hydrogen spillover configurations have also been calculated and confirmed that Fig. 5b is the most preferable hydrogen spillover configurations for single Pt atom. In fact, the spillover configuration Fig. 5b should be the ground state of Pt_1/H_Al_2O_3. Subsequently, the H desorption as $1/2H_2$ is endothermic by 1.45 eV. Herein, a question raised that why the H_3 is the most preferable hydrogen spillover site?

We further checked the hydrogen spillover of Pt_2/H_Al_2O_3 with H1–H4. The H1–H3 atoms derived from the dissociation of H_2O molecules and was located on the lattice O atoms of surface Al_2O_3 to form OH groups. The H4 is part of the OH group derived from the dissociated H_2O molecule. H4 was chosen because it was nearby the adsorbed Pt_2 cluster on the surface. The obtained configurations are shown in Fig. 6. For H1–H3, the spillover energies are increased as −0.43, −0.54 and −0.73 eV, respectively. The spillover energy for H4 spillover are −0.30 or −0.12 eV, both are less thermodynamically preferable than H1–H3. The H3 is still the most preferable spillover sites for Pt_2/H_Al_2O_3 as that for Pt_1/H_Al_2O_3. The corresponding net energies cost for the further desorption of H1–H4 in Fig. 6a–d are 1.06, 0.96, 0.89 (as shown in Fig. 6c*) and 1.15 eV, respectively. The lowest net energy needed is 0.89 eV for H3, which is 0.61 eV higher than that of Pt_1/H_Al_2O_3. Again, the spillover configuration should be the ground state of Pt_2/H_Al_2O_3 in the realistic reaction conditions, where the energy cost for H desorption as $1/2H_2$ is 1.62 eV.

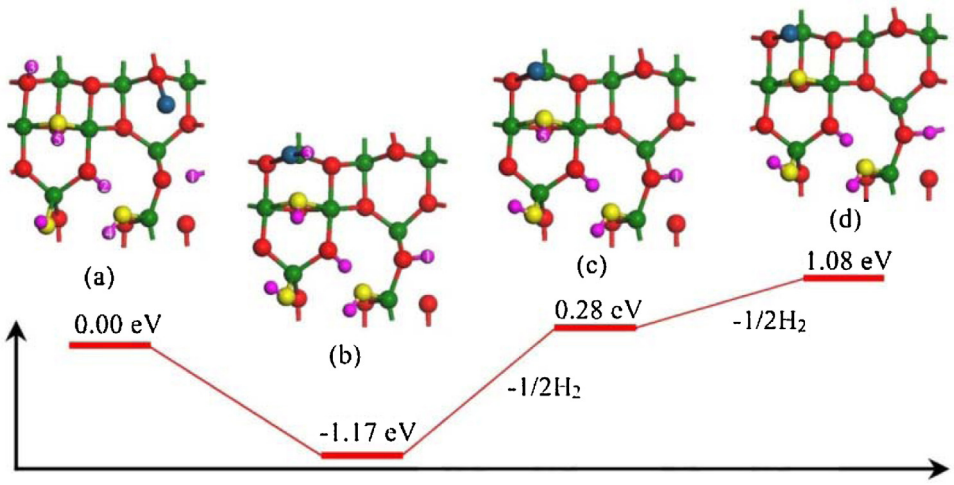

Fig. 5. Hydrogen spillover geometries and energy changes of Pt/H_Al_2O_3.

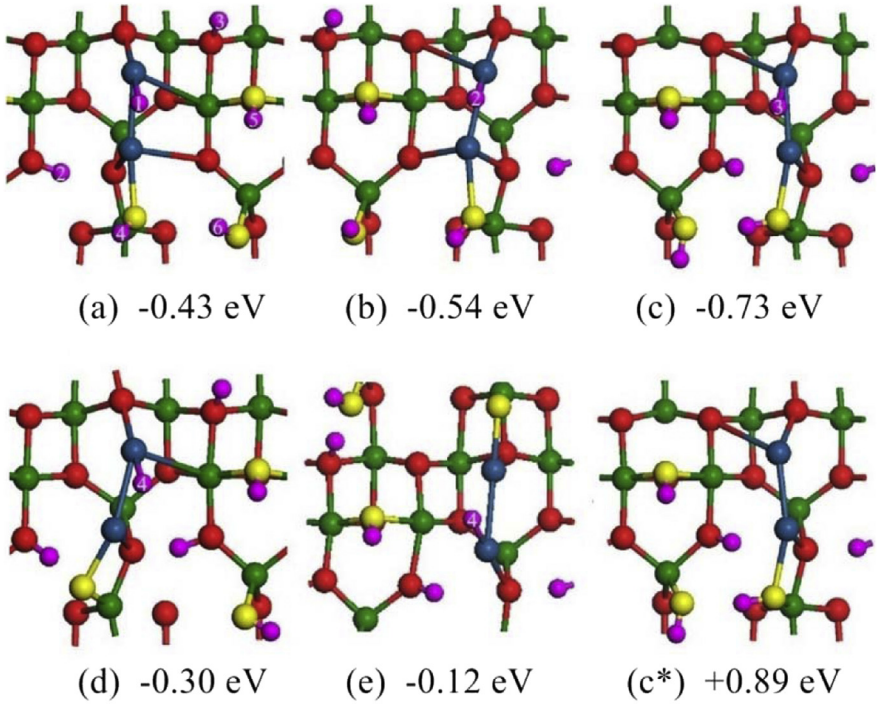

Fig. 6. Hydrogen spillover geometries of Pt_2/H_Al_2O_3. The energies labeled refer to the total energy of Pt_2/H_Al_2O_3.

Different from the situations of Pt_1/H_Al_2O_3 and Pt_2/H_Al_2O_3, the hydrogen spillover on Pt_3/H_Al_2O_3 is not thermodynamically preferable. For H1–H3, the spillover energies are positive 0.34, 0.21 and 0.01 eV respectively (see Table 3). The corresponding desorption energies cost for H atom as $1/2H_2$ molecule are 1.16, 1.06 and 0.85 eV. The initial adsorption configuration Fig. 3g is the ground state, not the spillover configurations in this situation. Additionally, the H3 is not only the most preferable spillover site, but also the desorption of H from the spillover configuration is the most economic thermodynamically. This is the same as that for Pt_2/H_Al_2O_3 and Pt_1/H_Al_2O_3.

Table 3
Energetic for H spillover and desorption of Pt_3/H_Al_2O_3.

Sites	H1	H2	H3
Spillover energy, eV	0.34	0.21	0.01
Desorption energy, eV	1.15	1.05	0.85

4. Discussions

The adsorption and growth of Pt_n cluster and hydrogen spillover on Pt_n/H_Al_2O_3 have been investigated above. There are two points that should be further spotlighted: (1) How does the support affect the adsorption and growth of Pt_n cluster of Pt_n/Al_2O_3 catalyst? (2) How do the support and size of Pt_n cluster affect the hydrogen spillover?

For the first point, no matter clean or hydrated, there is a "basin" structure on the surface of γ-Al_2O_3(1 1 0) that acts as a accepter for the location of Pt_n cluster. As Fig. 1c shown, the surface atoms Al_C, Al_D, O_5 and O_4 delineate the basin on the clean surface. The basin is just beside the only tri-coordinated Al_D cation in the surface. Due to the strong Lewis acidity of Al_D [19], the basin is suitable for

Table 4
Bader valence (BV) of H atoms and H–O bond lengths of H_Al_2O_3 surfaces with Pt_n supported or not.

H-sites	H_Al_2O_3		Pt_1/H_Al_2O_3		Pt_2/H_Al_2O_3		Pt_3/H_Al_2O_3		Pt_4/H_Al_2O_3	
	BV, eV	H–O, Å	BV, eV	H–O, Å	BV, eV	H–O, Å	BV, eV	H–O, Å	BV, eV	H–O, Å
H1	0.635	1.13	0.645	1.11	0.662	1.04	0.668	1.04	0.640	1.03
H2	0.659	1.07	0.644	1.06	0.616	1.02	0.547	1.04	0.604	1.01
H3	0.662	1.04	0.651	1.05	0.675	1.05	0.666	1.05	0.679	1.04
H4	0.621	0.99	0.605	0.99	0.614	0.98	0.620	0.98	0.611	1.00
H5	0.600	0.99	0.605	0.98	0.594	0.98	0.597	0.99	0.626	0.99
H6	0.615	0.98	0.628	0.98	0.619	0.98	0.635	0.98	0.615	0.98

the location of electrophilic groups or clusters. Subsequently, the interaction energy between the adsorbed Pt_n cluster and the basin is very strong, and became stronger as the size of cluster increases. During the hydration process, which usually happens in realistic reactions, OH group is prior to occupy the surface cations, particularly the tri-coordinated Al_D, and tetra-coordinated Al_C as well. The original basin was covered and a new one was created as shown in Fig. 1d, the basin O_1-Al_A-O_4-Al_B. As the loss of unsaturated coordination and tri-coordinated Al sites, the Lewis basicity of the new basin formed on hydrated surface is weaker than the one on clean surface, resulting in reducing both of the interaction energy and the electrons transfer. The surface OH groups also add the flexibility of the surface, which reduces the resistance to the aggregation of Pt_n cluster.

For the second point, it has been recognized that the H3 is the most feasible candidate for H spillover to supply H species for catalytic hydrogenation. To uncover this point, all the OH bond length of the hydrated γ-Al_2O_3(1 1 0) surface and the Bader valence of the H atoms have been collected and tabulated in Table 4. The bond lengths of OH groups 1–3 are 1.04–1.13 Å, comparing to 0.98–0.99 Å of OH groups 4–6. It should be noted that, the Bader valence of H3 is almost the largest one among the six H atoms, no matter on the hydrated surface or all the Pt_n/H_Al_2O_3 catalysts. It indicates that the H3 is the most ionized, and possesses the strongest Brønsted acidity [19]. On the other hand, the adsorbed Pt_n was charged by the hydrated surface (see Table 2) with electrons. The Coulomb interaction between the positive and negative charges could help to underlie why the H3 is the chosen one for hydrogen spillover.

On the basis of projected density of states (PDOS) analysis (Fig. 7), the intrinsic difference between the H3 and H4 was dug out. For the hydrated surface without Pt_n supported (Fig. 7a), there is an *s-p* hybridization in bottom of the valence band of the H3 PDOS, through which massive electrons was transferred from H3 to the tri-coordinated O_3 atom connected to it. The hybridization states exist as well for Pt_2/H_Al_2O_3 (Fig. 7b) and Pt_3/H_Al_2O_3 (Fig. 7c), and tends to shift to deep energy level. The decomposed charge densities of the *s-p* hybridization for H_Al_2O_3, Pt_1/H_Al_2O_3 and Pt_2/H_Al_2O_3 confirm that the H3 contributes most of the *s-p* hybridization. This unique electron structure of H3 would be ascribed to that it is the only hydrogen atom coordinated to the tri-coordinated surface oxygen atom in the topmost layer.

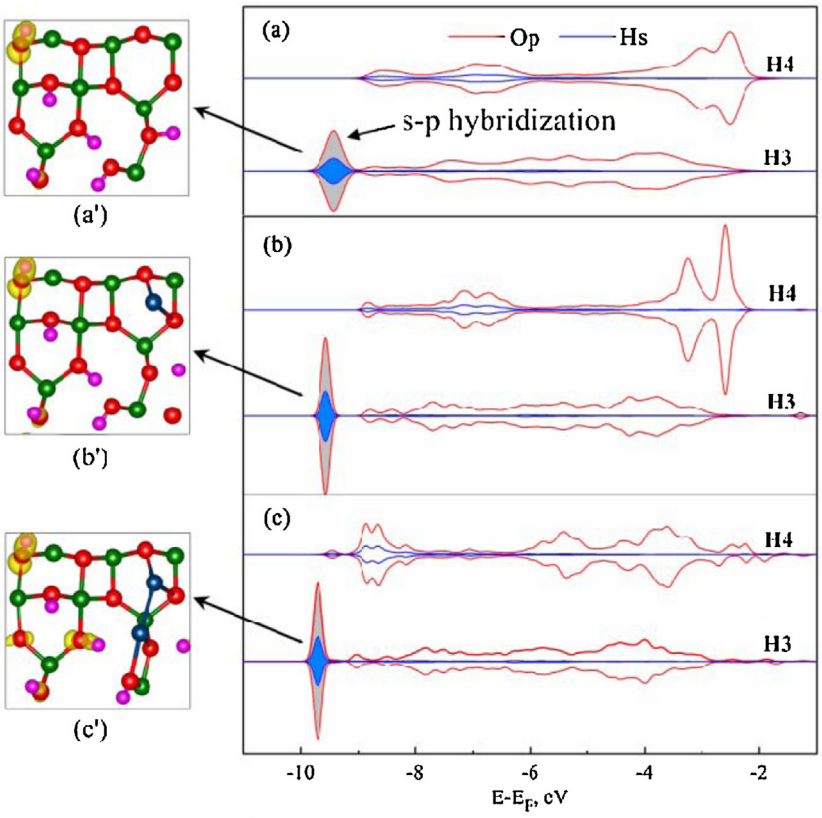

Fig. 7. PDOS of H atoms at site 3 and 4 of (a) H_Al_2O_3, (b) Pt_1/H_Al_2O_3 and (c) Pt_2/H_Al_2O_3 surfaces. Corresponding decomposed charge density of the *s-p* hybridization has been presented beside.

Energetic results indicate that, there are some dependences of the performance of H spillover on the size of Pt_n cluster. For $n = 1–2$, the H (H3) spillover is thermodynamically spontaneous and the spillover configurations was recognized as the ground state, not the original Pt_n supported structure. In this situation, the desorption energy of the H atom is 1.45 and 1.62 eV for $Pt_1/H\_Al_2O_3$ and $Pt_2/H\_Al_2O_3$ respectively, which could happen at a high temperature. While, for $n = 3$, the H spillover is not a thermodynamically spontaneous process any more. But, the spillover energy is as low as 0.01 eV for H3. A further energy cost for the desorption of H as $1/2H_2$ is 0.85 eV, which is about half of that needed for the cases $n = 1–2$. It could happen at a mild temperature. It comes to the end that, the $Pt_3/H\_Al_2O_3$ is more suitable to act as a hydrogen supplier than $Pt_1/H\_Al_2O_3$ and $Pt_2/H\_Al_2O_3$.

The high spillover energy release and low desorption energy cost of H3 on $Pt_3/H\_Al_2O_3$ could be ascribed to the interaction of Pt_3 cluster to the basin O_1-Al_A-O_4-Al_B on the surface of the support. When $n < 3$, the basin is too large to accommodate the clusters, which makes the Pt_n coordinated unsaturated seriously. Naturally, the spillover of H from the Al_2O_3 surface to the supported Pt_n cluster adds the stability of $Pt_n/H\_Al_2O_3$ structure, while the further desorption of H reduces it. When $n = 3$, the Pt_3 is well restricted in the basin and its coordination degree of saturation is increased by the third Pt atom, which makes it easy both for the H spillover and desorption. For H1 and H2, both the spillover energy and the desorption energy needed are obviously higher than that of H3. It denotes that the size of Pt_n cluster, together with the surface nature of the support, has complex impacts to the hydrogen spillover. The hydrogen spillover and desorption on $Pt_4/H\_Al_2O_3$ are not presented. But, in the same spirits, it could be expected that spillover energy will increase and the desorption energy will decrease. There would be an optimized size of Pt_n cluster, of which the desorption energy is decreased to a value equivalent to that of hydrogen spillover.

5. Conclusion

The adsorption and growth of small Pt_n ($n = 1–4$) cluster and hydrogen spillover on γ-Al_2O_3 surfaces have been investigated within the framework of density functional theory. A basin structure on both of the clean and hydrated surface was found to stabilize the Pt clusters. For the hydrated surface, the basin structure, together with the size of Pt_n cluster and unique nature of the support, was also found to take trivial impacts on the hydrogen spillover. The hydrogen located at the tri-coordinated O atoms in the topmost surface of γ-Al_2O_3(1 1 0) was identified to be the most effective hydrogen supplier. This has been ascribed to the unique *s-p* hybridization of the H and O atoms at the site. Based on the balancing on the energy cost for hydrogen spillover and desorption, the Pt_n ($n = 3–4$) was found to be much more active than Pt_n ($n = 1–2$) in the range of Pt_n size we investigated. It implies there would be an optimized size of the supported Pt_n cluster at $n > 3$.

Acknowledgement

This work was financially supported by Science and Technology Department of Sichuan Province (2012FZ0009) and Chengdu Guohua Environment Protection Science and Technology Co. Ltd. We also acknowledge the National Supercomputing Center in Shenzhen for computational service support.

References

[1] S. Aranifard, S.C. Ammal, A. Heyden, On the importance of metal-oxide interface sites for the water-gas shift reaction over Pt/CeO_2 catalysts, J. Catal. 309 (2014) 314–324.
[2] S. Wang, K.H. Yin, Y.C. Zhang, H.C. Liu, Glycerol hydrogenolysis to propylene glycol and ethylene glycol on zirconia supported noble metal catalysts, ACS Catal. 3 (2013) 2112–2121.
[3] M.C. Valero, P. Raybaud, P. Sautet, Interplay between molecular adsorption and metal-support interaction for small supported metal clusters: CO and C_2H_4 adsorption on Pd_4/γ-Al_2O_3, J. Catal. 247 (2007) 339–355.
[4] S.Y. Wu, Y.R. Lia, J.J. Ho, H.M. Hsieh, Density functional studies of ethanol dehydrogenation on a $2Rh/\gamma$-Al_2O_3(1 1 0) surface, J. Phys. Chem. C 113 (2009) 16181–16187.
[5] J.M.H. Lo, T. Ziegler, P.D. Clark, SO_2 adsorption and transformations on γ-Al_2O_3 surfaces: a density functional theory study, J. Phys. Chem. C 114 (2010) 10444–10454.
[6] L. Cui, Y. Tang, H. Zhang, L.G.J. Hector, C. Ouyang, S. Shi, H. Li, L. Chen, First-principles investigation of transition metal atom M (M = Cu, Ag, Au) adsorption on CeO_2(1 1 0), Phys. Chem. Chem. Phys. 14 (2012) 1923–1933.
[7] P. Raybaud, C. Chizallet, C. Mager-Maury, M. Digne, H. Toulhoat, P. Sautet, From γ-alumina to supported platinum nanoclusters in reforming conditions: 10 years of DFT modeling and beyond, J. Catal. 308 (2013) 328–340.
[8] H.J. Sedjame, C. Fontaine, G. Lafaye, J. Barbier Jr., On the promoting effect of the addition of ceria to platinum based alumina catalysts for VOCs oxidation, Appl. Catal. B: Environ. 144 (2014) 233–242.
[9] A. Ishikawa, E. Iglesia, Bifunctional pathways mediated by Pt clusters and Al_2O_3 in the catalytic combustion of dimethyl ether, Chem. Commun. (2007) 2992–2993.
[10] S. Vajda, M.J. Pellin, J.P. Greeley, C.L. Marshall, L.A. Curtiss, G.A. Ballentine, J.W. Elam, S. Catillon-Mucherie, P.C. Redfern, F. Mehmood, P. Zapol, Subnanometre platinum clusters as highly active and selective catalysts for the oxidative dehydrogenation of propane, Nat. Mater. 8 (2009) 213–216.
[11] R. Prins, V.K. Palfi, M. Reiher, Hydrogen spillover to nonreducible supports, J. Phys. Chem. C 116 (2012) 14274–14283.
[12] S. Khoobiar, Particle to particle migration of hydrogen atoms on platinum-alumina catalysts from particle to neighboring particles, J. Phys. Chem. 68 (1964) 411–412.
[13] Y.X. Pan, C.J. Liu, Q.F. Ge, Effect of surface hydroxyls on selective CO_2 hydrogenation over Ni_4/γ-Al_2O_3: a density functional theory study, J. Catal. 272 (2010) 227–234.
[14] B. Hvolbæk, T.V.W. Janssens, B.S. Clausen, H. Falsig, C.H. Christensen, J.K. Nøskov, Catalytic activity of Au nanoparticles, Nanotoday 2 (2007) 14–18.
[15] F. Behafarid, L.K. Ono, S. Mostafa, J.R. Croy, G. Shafai, S. Hong, T.S. Rahman, S.R. Bare, B.R. Cuenya, Electronic properties and charge transfer phenomena in Pt nanoparticles on γ-Al_2O_3: size, shape, support, and adsorbate effects, Phys. Chem. Chem. Phys. 14 (2012) 11766–11779.
[16] H.T. Wang, L.J. Chen, Y.K. Lv, R.P. Ren, H_2 dissociation on γ-Al_2O_3 supported Cu/Pd atoms: A DFT Investigation, Appl. Surf. Sci. 290 (2014) 154–160.
[17] T.Q. Nguyen, E.M.C. Sison, N. Hiroshi, K. Hideaki, M. Hiroyoshi, O. Kazuo, S. Kaoru, DFT Plus U study on the oxygen adsorption and dissociation on CeO_2-supported platinum cluster, Appl. Surf. Sci. 288 (2014) 244–250.
[18] D. Mei, J.H. Kwak, J. Hu, S.J. Cho, J. Szanyi, L.F. Allard, C.H.F. Peden, Unique role of anchoring penta-coordinated Al^{3+} sites in the sintering of γ-Al_2O_3-supported Pt catalysts, J. Phys. Chem. Lett. 1 (2010) 2688–2691.
[19] M. Digne, P. Sautet, P. Raybaud, P. Euzen, H. Toulhoat, Use of DFT to achieve a rational understanding of acid-basic properties of γ-alumina surfaces, J. Catal. 226 (2004) 54–68.
[20] M. Digne, P. Sautet, P. Raybaud, P. Euzen, H. Toulhoat, Hydroxyl groups on γ-alumina surfaces: A DFT Study, J. Catal. 211 (2002) 1–5.
[21] Y.X. Pan, C.J. Liu, Q.F. Ge, Adsorption and protonation of CO_2 on partially hydroxylated γ-Al_2O_3 surfaces: a density functional theory study, Langmuir 24 (2008) 12410–12419.
[22] S.X. Yin, T. Swift, Q.F. Ge, Adsorption and activation of CO_2 over the Cu–Co catalyst supported on partially hydroxylated γ-Al_2O_3, Catal. Today 165 (2011) 10–18.
[23] J. Li, R. Zhang, B. Wang, Influence of the hydroxylation of γ-Al_2O_3 surfaces on the stability and growth of Cu for Cu/γ-Al_2O_3 catalyst: A DFT Study, Appl. Surf. Sci. 270 (2013) 728–736.
[24] X.R. Shi, D.S. Sholl, Nucleation of Rh_n ($n = 1–5$) clusters on γ-Al_2O_3 surfaces: A Density Functional Theory Study, J. Phys. Chem. C 116 (2012) 10623–10631.
[25] R.G. Zhang, B.J. Wang, H.Y. Liu, L.X. Ling, Effect of surface hydroxyls on CO_2 hydrogenation over Cu/γ-Al_2O_3: a theoretical study, J. Phys. Chem. C 115 (2011) 19811–19818.
[26] Y.X. Pan, C.J. Liu, T.S. Wiltowski, Q. Ge, CO_2 adsorption and activation over γ-Al_2O_3-supported transition metal dimers: a density functional study, Catal. Today 147 (2009) 68–76.
[27] G. Feng, C.F. Huo, C.M. Deng, L. Huang, Y.W. Li, J. Wang, H. Jiao, Isopropanol adsorption on γ-Al_2O_3 surfaces: a computational study, J. Mol. Catal. A: Chem. 304 (2009) 58–64.
[28] G. Feng, C.F. Huo, Y.W. Li, J. Wang, H. Jiao, Structures and energies of iron promoted γ-Al_2O_3 surface: a computational study, Chem. Phys. Lett. 510 (2011) 224–227.
[29] J.P. Perdew, K. Burke, M. Ernzerhof, Generalized gradient approximation made simple, Phys. Rev. Lett. 77 (1996) 3865–3868.
[30] G. Kresse, J. Furthmüller, Efficient iterative schemes for ab initio total-energy calculations using a plane-wave basis set, Phys. Rev. B 54 (1996) 11169–11186.

[31] G. Kresse, J. Furthmüller, Efficiency of ab-initio total energy calculations for metals and semiconductors using a plane-wave basis set, Comput. Mater. Sci. 6 (1996) 15–50.
[32] G. Kresse, D. Joubert, From Ultrasoft pseudopotentials to the projector augmented-wave method, Phys. Rev. B 59 (1999) 1758–1775.
[33] M. Teliska, V.S. Murthi, S. Mukerjee, D.E. Ramaker, Correlation of water activation, surface properties, and oxygen reduction reactivity of supported Pt–M/C bimetallic electrocatalysts using XAS, J. Electrochem. Soc. 152 (2005) A2159–A2169.
[34] S.I. Sanchez, L.D. Menard, A. Bram, J.H. Kang, M.W. Small, R.G. Nuzzo, A.I. Frenkel, The emergence of nonbulk properties in supported metal clusters: negative thermal expansion and atomic disorder in Pt nanoclusters supported on γ-Al_2O_3, J. Am. Chem. Soc. 131 (2009) 7040–7054.
[35] M.C. Valero, P. Raybaud, P. Sautet, Nucleation of Pd_n (n = 1–5) clusters and wetting of Pd particles on γ-Al_2O_3 surfaces: a density functional theory study, Phys. Rev. B 75 (2007) 045427.
[36] Z. Liu, Y. Wang, J. Li, R. Zhang, The effect of γ-Al_2O_3 surface hydroxylation on the stability and nucleation of Ni in Ni/γ-Al_2O_3 catalyst: a theoretical study, RSC Adv. 4 (2014) 13280–13292.
[37] X.S. Liu, DRIFTS study of surface of γ-alumina and its dehydroxylation, J. Phys. Chem. C 112 (2008) 5066–5073.
[38] R. Bader, Atoms in molecules: a quantum theory, Oxford University Press, 1994.
[39] R. Zhang, H. Liu, B. Wang, L. Ling, Insights into the effect of surface hydroxyls on CO_2 hydrogenation over Pd/γ-Al_2O_3 catalyst: a computational study, Appl. Catal. B: Environ. 126 (2012) 108–120.